Journal of Photochemistry and Photobiology A: Chemistry 356 (2018) 700–707

Contents lists available at ScienceDirect

Journal of Photochemistry and Photobiology A: Chemistry

journal homepage: www.elsevier.com/locate/jphotochem

Spectroscopic properties of a chromone-fluorescein conjugate as Mg^{2+} "turn on" fluorescent probe

Chao-rui Li[a], Si-liang Li[a,b], Guan-qun Wang[a], Zheng-yin Yang[a,*]

[a] College of Chemistry and Chemical Engineering, State Key Laboratory of Applied Organic Chemistry, Lanzhou University, Lanzhou 730000, PR China
[b] School of Petrochemical Engineering, Lanzhou University of Technology, Lanzhou 730050, PR China

ARTICLE INFO

Article history:
Received 29 September 2015
Received in revised form 18 February 2016
Accepted 1 March 2016
Available online 26 April 2016

Keywords:
Fluorescein
Fluorescent probe
Magnesium ion
Selectivity
Sensitivity

ABSTRACT

In this study, a novel fluorescein-derived Schiff-base ligand bearing a chromone moiety which was called 6-Hydroxy-3-formylchromone fluorescein hydrazone (**1**) has been designed, synthesized and evaluated as a Mg^{2+} "turn on" fluorescent probe. This probe **1** exhibited high selectivity and sensitivity towards Mg^{2+} over other important metal ions investigated, and the remarkable enhancement in fluorescence emission centered at 504 nm was observed in the presence of Mg^{2+}, which was attributed to the ring-opening process of the fluorescein fluorophore in probe **1** upon complexation of **1** with Mg^{2+}. Furthermore, the "turn on" response of this probe **1** to Mg^{2+} was nearly completed within 3 min, which indicated that this probe **1** could be utilized to sense and monitor Mg^{2+} for real-time detection.

1. Introduction

Recently, the interest in the development of highly selective and sensitive methods for detecting and monitoring metal ions has been a current thrust in the active research fields [1–5]. Among a variety of environmentally and biologically important metals, widespread applications of magnesium are found in many fields, such as aircraft industry [6], optical instruments [7], photographic technique [8] and alloy metals [9]. It is well known that magnesium is the eighth most abundant element on the earth's crust and the fourth most abundant cation in the human body [10]. Mg^{2+} is widely distributed in the macronutrient in the bone and plays a crucial role in various biological processes like bone remodeling [11], skeletal development [12], DNA synthesis [13] and signal transduction [14]. Furthermore, Mg^{2+} is also required for the proper functioning of central nervous systems and immune systems [15,16]. The regulated amounts of Mg^{2+} are beneficial to human health [17], but the deficiency of Mg^{2+} can lead to serious problems including skeletal, neurogenic, gastrointestinal and renal losses [18–21], causing some chronic diseases like osteoporosis [22], hypertension [23], coronary heart disease [24] and diabetes [25]. Therefore, it is desirable to develop a simple and rapid method to detect and sense Mg^{2+} in biological assays [26].

Among various detecting techniques for metal ion monitoring, fluorescence detection has attracted broad interests among scientists due to its relevant advantages, such as simplicity, high sensitivity, inexpensive apparatus, real-time detection and non-destructive property [27–29]. In the past decades, a number of Mg^{2+} selective and sensitive fluorescent probes have been reported [30–32], but some are suffering from interferences from other important biological species, especially Ca^{2+}, which is in the same group as Mg^{2+} in the periodic table, and has similar spectroscopic properties with Mg^{2+} [33]. Thus, it is of great challenge to design and synthesize Mg^{2+} fluorescent probes with high selectivity and sensitivity in the presence of other environmentally and biologically important metal ions [34].

Fluorescein and its derivatives have been extensively used as organic dyes to design fluorescent probes, labels and immunological probes by chemists and biologists, because of their excellent photophysical properties, such as long absorption and emission wavelength, large absorption coefficient, high fluorescent quantum yield and great photostability [35,36]. In recent years, several fluorescein-derived fluorescent probes that were designed and synthesized to recognize metal ions like Fe^{3+}, Cu^{2+}, Zn^{2+}, Hg^{2+} and Mg^{2+} have been studied [37–41]. It is well known that these fluorescein-derived fluorescent probes exist in a spirocyclic form, which is colorless and non-fluorescent. However, when a specific metal ion is added, the ring-opening process of the fluorescein moiety can be observed upon complexation of this probe with this metal ion, which results in the appearance of color and fluorescence [42].

Owing to their excellent spectroscopic and pharmacological properties, chromone-based compounds have been widely applied in antitumoral agents, cardio cerebrovascular drugs and fluorophores [43]. Bearing these in mind, we have designed and

* Corresponding author.
E-mail address: yangzy@lzu.edu.cn (Z.-y. Yang).

http://dx.doi.org/10.1016/j.jphotochem.2016.03.001
1010-6030/

synthesized a novel fluorescein-derived fluorescent probe bearing the chromone moiety which was called 6-Hydroxy-3-formylchromone fluorescein hydrazone (**1**) (Scheme 1). This probe showed high selectivity and sensitivity for Mg^{2+} with remarkable fluorescence enhancement centered at 504 nm based on the ring-opening process of the fluorescein moiety in ethanol, but the fluorescence emission intensity was decreased to a certain degree with addition of water. Hence, this probe could be utilized to detect and recognize Mg^{2+} using fluorescein moiety as a fluorophore in ethanol.

2. Experimental

2.1. Materials

Hydroquinone, acetic anhydride, concentrated sulfuric acid, aluminum chloride, phosphorus oxychloride, fluorescein, hydrazine hydrate, ethyl acetate, absolute ethanol, N,N-dimethyl formamide (DMF), anhydrous sodium sulfate and salts of Mg^{2+}, Al^{3+}, Ba^{2+}, Ca^{2+}, Cd^{2+}, Co^{2+}, Cr^{3+}, Cu^{2+}, Fe^{2+}, Fe^{3+}, K^{+}, Mn^{2+}, Na^{+}, Ni^{2+}, Pb^{2+} and Zn^{2+} were obtained from commercial suppliers, and used as received without further purification. Stock solution of compound **1** (10 mM) was prepared in absolute ethanol. Stock solutions (10 mM) of the salts of Mg^{2+}, Al^{3+}, Ba^{2+}, Ca^{2+}, Cd^{2+}, Co^{2+}, Cr^{3+}, Cu^{2+}, Fe^{2+}, Fe^{3+}, K^{+}, Mn^{2+}, Na^{+}, Ni^{2+}, Pb^{2+} and Zn^{2+} in absolute ethanol were also prepared. Distilled water was used throughout all experiments.

2.2. Apparatus

^{1}H NMR spectra were recorded on the JNM-ECS 400 MHz instruments spectrometers using TMS (tetramethylsilane) as an internal standard and DMSO-*d* as a solvent. The ESI–MS data were obtained in ethanol from a Bruke Esquire 6000 spectrometer. UV–vis absorption spectra were collected on a Shimadzu UV-240 spectrophotometer. Fluorescence measurements were performed on a Hitachi RF-5301 fluorimeter equipped with quartz cuvettes of 1 cm path length at 298 K. Melting points were determined on a Beijing XT4-100x microscopic melting point apparatus without correction.

2.3. Synthesis

Hydroquinone diacetate (**2**), acetylquinol (**3**) and 6-hydroxy-3-formylchromone (**4**) were synthesized according to the reported methods [44]. The synthetic route of compound **1** was shown in Scheme 1.

2.3.1. Synthesis of compound *5* (Fluorescein hydrazine)

Fluorescein (1.25 g, 3.75 mmol) was dissolved in absolute ethanol (30 mL) and hydrazine hydrate (2.0 mL, 2.06 g, 41.28 mmol) was added to the orange red solution above. The mixture was refluxed for 18 h under stirring, during which time the color of fluorescein disappeared. After the reaction was completed, the reaction mixture was cooled to room temperature, and poured into ethyl acetate (100 mL). Then the mixture was washed with distilled water for 6 times and the organic layer was dried with anhydrous sodium sulfate. After filteration to remove anhydrous sodium sulfate, the filtrate was evaporated under reduced pressure. The obtained solid was recrystallized from absolute ethanol (30 mL) to give compound **5** as a pale yellow powder (Scheme 1). Yield: 0.67 g (51.59%). m.p. 248–250 °C, ^{1}H NMR (400 MHz, DMSO-*d*) (Fig. S1): 9.65 (s, 2H, −OH), 7.79-7.73 (m, 1H, H_7), 7.51-7.45 (m, 2H, $H_{4,5}$), 7.00-6.94 (m, 1H, H_6), 6.59 (d, 2H, J = 2.4 Hz, H_1), 6.45 (dd, 2H, J = 8.8 Hz, J = 2.4 Hz, H_2), 6.40 (d, 2H, J = 8.8 Hz, H_3), 4.27 (s, 2H, $-NH_2$). MS (ESI) (Fig. S2): *m/z* $[M+H^+]^+$ calcd 347.3265, found 347.0830; $[M+Na^+]^+$ calcd 369.3084, found 369.0626.

2.3.2. Synthesis of compound *1* (6-Hydroxy-3-formylchromone fluorescein hydrazone)

A solution of fluorescein hydrazine (**5**) (0.328 g, 0.948 mmol) in absolute ethanol (30 mL) was added dropwise to another solution containing 6-Hydroxy-3-formylchromone (**4**) (0.180 g, 0.948 mmol) in absolute ethanol (30 mL) under stirring. The mixture was refluxed for 13 h under stirring, and then cooled to room temperature. The reaction mixture was poured into distilled water (50 mL) and an earth yellow solid was separated out from the solution. Then the solid was filtered under reduced pressure, washing five times with distilled water (10 mL). The obtained crude product was recrystallized from absolute ethanol (30 mL) to afford the desired product **1** as an earth yellow powder (Scheme 1). Yield: 0.38 g (77.38%). m.p. 259–261 °C, ^{1}H NMR (400 MHz, DMSO-*d*) (Fig. S3): 10.14 (s, 1H, $-OH_{chromone}$), 9.95 (s, 2H, $-OH_{fluorescein}$), 8.71 (d, 1H, J = 0.8 Hz, H_8), 8.32 (d, 1H, J = 0.8 Hz, −CH=N-), 7.93 (dt, 1H, J = 7.2 Hz, J = 0.8 Hz, H_7), 7.63 (td, 1H, J = 7.2 Hz, J = 0.8 Hz, H_5), 7.58 (td, 1H, J = 7.2 Hz, J = 0.8 Hz, H_6), 7.51 (d, 1H, J = 9.2 Hz, H_9), 7.27 (d, 1H, J = 3.2 Hz, H_{11}), 7.22 (dd, 1H, J = 9.2 Hz, J = 3.2 Hz, H_{10}), 7.09 (dt, 1H, J = 7.2 Hz, J = 0.8 Hz, H_4), 6.67 (d, 2H, J = 2.0 Hz, H_1), 6.50 (d, 2H, J = 8.4 Hz, H_3), 6.46 (dd, 2H, J = 8.4 Hz, J = 2.0 Hz, H_2). MS (ESI) (Fig. S4): *m/z* $[M+H^+]^+$ calcd 519.4583, found 519.1340; $[M+Na^+]^+$ calcd 541.4401, found 541.1175.

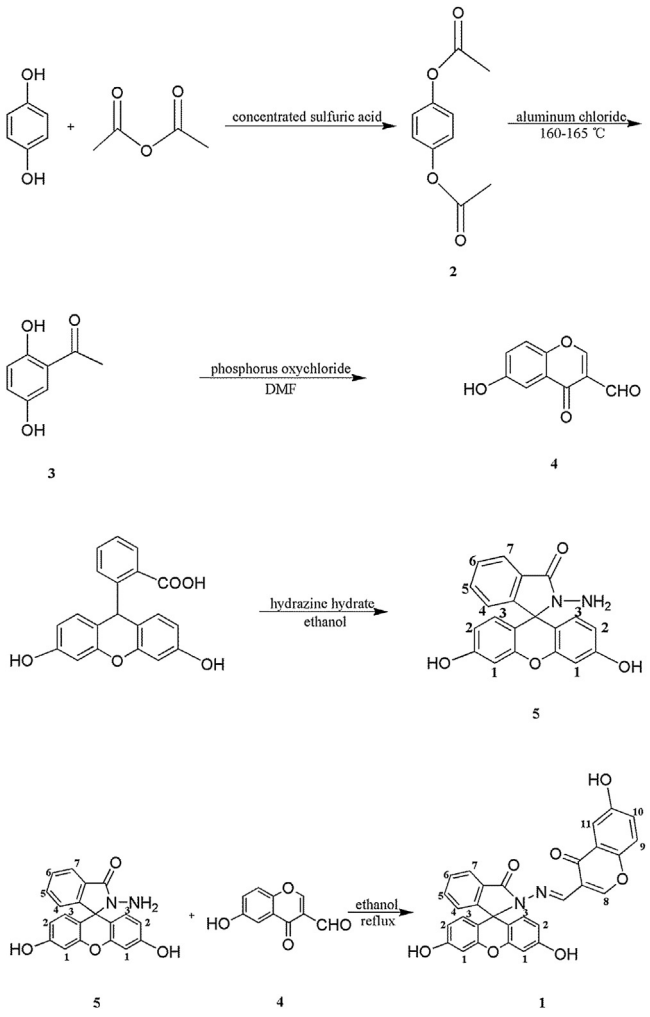

Scheme 1. The synthetic route of compound 1.

2.4. General information

Test solutions were prepared by placing 10 μL of the probe stock solution into cuvettes, adding an appropriate aliquot of each metal ion stock, and diluting the solution to 2 mL with ethanol. For all fluorescence measurements of compound **1**, the fluorescence intensity of the test solution was recorded at 504 nm, and the excitation wavelength was set at 323 nm. The excitation and emission slit widths were both 3 nm in fluorescence emission spectra of **1**.

The binding constant value for complex **1**-Mg^{2+} was determined on the basis of the nonlinear filtting of the fluorescence titration curve assuming a 2: 1 stoichiometry by the Benesi–Hildebrand method (1) [45,46]:

$$\frac{1}{F - F_{min}} = \frac{1}{K - \left(F_{max} - F_{min}\right)[Mg^{2+}] + \frac{1}{(F - F_{min})}} \quad (1)$$

Where F_{min}, F, and F_{max} are the emission intensities of the organic moiety considered in the absence of magnesium ion, at an intermediate magnesium concentration, and at a concentration of complete interaction, respectively, and where *K* is the binding constant concentration.

The detection limit was estimated from the fluorescence titration. The emission intensity of compound **1** without any anion was measured to determine the S/N ratios [47,48], and the standard deviation of blank measurements was calculated. The detection limit was calculated based on $3 \times \sigma_{blank}/k$, where σ_{blank} is the standard deviation of the blank solution and k is the slope of the calibration plot.

3. Results and discussion

3.1. Synthesis and characterization of compound *1*

Compound **1** was synthesized according to the synthetic route outlined in Scheme 1. Hydroquinone diacetate (**2**), acetylquinol (**3**) and 6-hydroxy-3-formylchromone (**4**) were synthesized according to the reported methods [44]. Fluorescein hydrazine (**5**) was prepared by reacting fluorescein with hydrazine hydrate under refluxing in absolute ethanol. Then the reaction between fluorescein hydrazine (**5**) and 6-hydroxy-3-formylchromone (**4**) in absolute ethanol afforded compound **1** as an earth yellow powder. The structure of compound **1** was characterized by ^1H NMR and mass spectrometry. The details of the characterization data of intermediate product and compound **1** were presented in the Supporting Information (Fig. S1–S4).

3.2. UV–vis titration of compound *1* with various amounts of Mg^{2+}

Firstly, we examined the UV–vis titration spectra of compound **1** in the presence of various amounts of Mg^{2+} in ethanol and the results were shown in Fig. 1. The free compound **1** exhibited three weak bands centered at 224 nm, 283 nm and 332 nm (Fig. S5), which were probably assignable to chromone moiety. However, upon addition of increasing amounts of Mg^{2+}, the gradual enhancement in the absorbance of this three bands was observed. Simultaneously, a new intense peak at 426 nm with two shoulders at 408 nm and 449 nm which was ascribed to fluorescein fluorophore appeared with increasing absorbance (Fig. 1). This phenomenon was attributed to the ring-opening process of the fluorescein fluorophore upon complexation of compound **1** with Mg^{2+}, which led to the UV–vis absorption enhancement. From the results above, it was concluded that the chromone unit and fluorescein moiety in compound **1** participated in the coordination with Mg^{2+}.

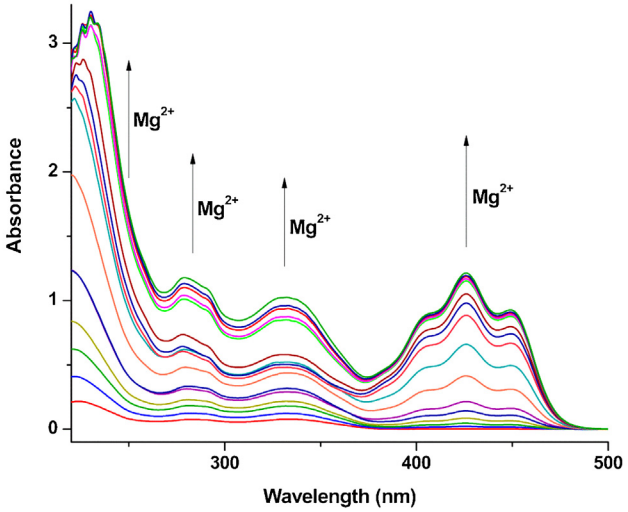

Fig. 1. Change in UV–vis absorption spectra of 1 (100 μM) upon addition of various amounts of Mg^{2+} (0.2, 0.4, 0.6, 0.8, 1.0, 1.2, 1.4, 1.6, 1.8, 2.0, 2.4, 2.8, 3.2, 3.6, 4.0 *equiv.*, respectively) in ethanol.

3.3. Fluorescence performance of compound *1* for sensing Mg^{2+}

The influence of reaction time on the fluorescence emission response of compound **1** to Mg^{2+} was conducted to determine if this compound **1** could be utilized as a Mg^{2+} fluorescent probe for real-time detection. For this purpose, the fluorescence emission intensity at 504 nm was recorded at different time in ethanol solution of a mixture of **1** and Mg^{2+} (1.0 *equiv.*). As shown in Fig. S6, the reaction process between compound **1** and Mg^{2+} was nearly completed within 3 min and the fluorescence emission intensity at 504 nm did not change further with more reaction time (Fig. S6), which demonstrated that this compound **1** could be used as a Mg^{2+} fluorescent probe for real-time detection. Interestingly, because Ca^{2+} may coordinate with compound **1**, we also conducted the effect of reaction time on the fluorescence emission response of **1** to Ca^{2+}. During this experimental process, little enhancement in fluorescence emission intensity at 504 nm was observed in the presence of 1.0 *equiv.* of Ca^{2+}, and the reaction was nearly completed within 2 min (Fig. S7), which indicated that this compound **1** had high selectivity towards Mg^{2+} over Ca^{2+} and could also respond to Ca^{2+} rapidly.

The changes in fluorescence emission spectra of compound **1** in the presence of various respective metal ions (Mg^{2+}, Al^{3+}, Ba^{2+}, Ca^{2+}, Cd^{2+}, Co^{2+}, Cr^{3+}, Cu^{2+}, Fe^{2+}, Fe^{3+}, K^{+}, Mn^{2+}, Na^{+}, Ni^{2+}, Pb^{2+}, Zn^{2+}) were then explored in ethanol and the results were depicted in Fig. 2 (a). Upon excitation of the chromone moiety at 323 nm, compound **1** in the absence of any metal ion displayed nearly no fluorescence emission in the range of 410–640 nm. Nevertheless, significant enhancement in fluorescence emission intensity at 504 nm was observed in the presence of Mg^{2+}. Interestingly, the addition of Zn^{2+} into the solution of compound **1** showed similar fluorescence response with that of Mg^{2+}, but the intensity was relatively low (Fig. 2 (b)). However, the addition of other metal ions investigated, especially Ca^{2+}, caused almost no change in fluorescence emission spectra (Fig. 2 (a)), which indicated that the selectivity of compound **1** was high for detecting and monitoring Mg^{2+}.

To obtain insight into the spectroscopic properties of compound **1** towards Mg^{2+} in the presence of various metal ions, competition experiments were carried out by adding these metal ions into the ethanol solution of **1**-Mg^{2+}. As illustrated in Fig. S8, the fluorescence

intensity of **1**-Mg^{2+} at 504 nm quenched significantly in the presence of Al^{3+}, Co^{2+}, Cr^{3+}, Cu^{2+}, Fe^{2+}, Fe^{3+} and Ni^{2+}, which was due to the formation of the complexes between ligand **1** and these metal ions, leading to the electron and energy transfer processes from ligand **1** to them [49–51]. However, these metal ions were present in relatively low concentrations in living systems [52]. Nevertheless, when other metal ions tested were added to the solution of **1**-Mg^{2+}, almost no change in fluorescence intensity at 504 nm were observed (Fig. S8). Thus, compound **1** could be utilized as a fluorescent probe for recognizing Mg^{2+} in the presence of most interfering metal ions in human body.

The fluorescence emission spectra of compound **1** towards increasing amounts of Mg^{2+} was then examined in ethanol and the results were illustrated in Fig. 3. With excited at 323 nm, nearly no fluorescence emission was observed in free **1**. It was probably due to the spirocyclic structure of the fluorescein moiety in compound **1**, which was non-fluorescent [53]. Nevertheless, the fluorescence emission centered at 504 nm enhanced gradually with increasing amounts of Mg^{2+}, and reached a plateau in the presence of 0.5 *equiv.* of Mg^{2+} (Fig. 3), which indicated that compound **1** formed a 2: 1 complex with Mg^{2+}. The reason was attributed to the ring-opening process of the fluorescein moiety upon complexation of **1** with Mg^{2+}, which resulted in the remarkable fluorescence enhancement [54–57] (Scheme 2). Furthermore, the detection limit of compound **1** for sensing Mg^{2+} was calculated based on the fluorescence titration spectra. As shown in Fig. 4, the fluorescence enhancement could be easily detected when the concentration of Mg^{2+} reached 0.05-0.50 μM, and a linear relationship between the fluorescence intensity at 504 nm and Mg^{2+} concentration was obtained in the range of 0.05-0.40 μM (Fig. S9). On a basis of the results above, the detection limit was calculated to be 2.67×10^{-8} M (0.64 ppb). As a result, the fluorescence emission intensity at 504 nm increased by about 49.58-fold in the presence of 0.5 *equiv.* of Mg^{2+} with high selectivity and sensitivity.

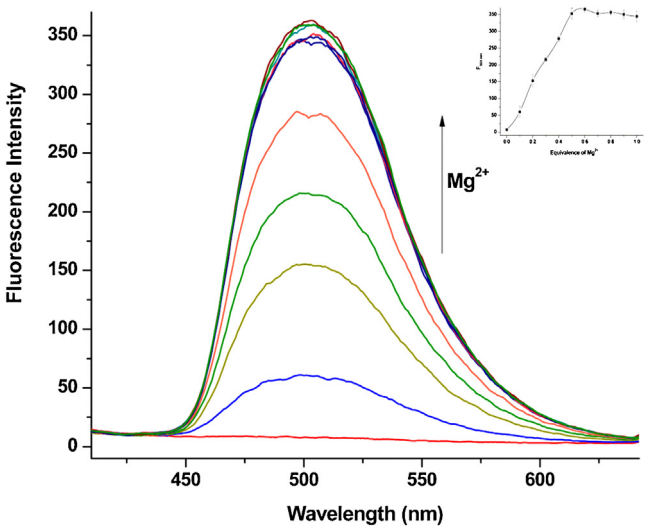

Fig. 3. Fluorescence emission spectra of 1 (50 μM) in the presence of increasing amounts of Mg^{2+} (0.1, 0.2, 0.3, 0.4, 0.5, 0.6, 0.7, 0.8, 0.9, 1.0 *equiv.*, respectively) in ethanol with an excitation at 323 nm. Insert: A linear calibration curve of the fluorescence emission intensity at 504 nm versus the concentration of Mg^{2+} over the range 0–50 μM.

3.4. Binding stoichiometry between compound *1* and Mg^{2+}

In order to confirm the binding stoichiometry between compound **1** and Mg^{2+} in ethanol, a Job's plot was conducted by keeping the total concentration of **1** and Mg^{2+} constant at 100 μM. As can be seen from Fig. 5, the fluorescence emission intensity at 504 nm was dependent on the molar ratio of Mg^{2+} in complex **1**-Mg^{2+} in the range of 0.1–0.9, and it reached maximum at the molar ratio of 0.3 (Fig. 5). These results suggested that a 2: 1 complex was formed between compound **1** and Mg^{2+}.

Moreover, in order to prove the binding stoichiometry between compound **1** and Mg^{2+}, the electrospray ionization mass spectra (ESI–MS) of complex **1**-Mg^{2+} was further explored by adding Mg $(NO_3)_2 \cdot 6H_2O$ into the ethanol solution of compound **1**. As depicted in Fig. 6, the peak at *m*/*z* 1123.6156 that was assignable to $[2\cdot\mathbf{1} + Mg^{2+} + C_2H_5OH + H_2O - H^+]^+$ (calcd *m*/*z* 1124.2812) was observed in the spectra, which proved the 2: 1 stoichiometry between compound **1** and Mg^{2+}. Based on the results of fluorescence titration spectra, Job's

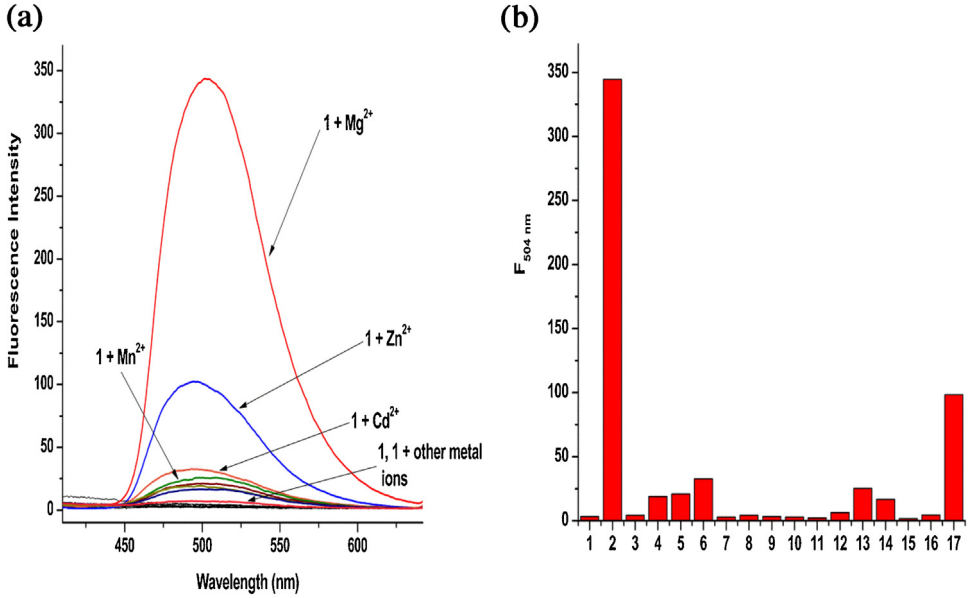

Fig. 2. (a) Changes in fluorescence emission spectra of 1 (50 μM) upon addition of Mg^{2+} (1 *equiv.*) and other respective metal ions (5 *equiv.*) in ethanol with an excitation at 323 nm. (b) The fluorescence intensities at 504 nm of 1 (50 μM) in the presence of Mg^{2+} (1 *equiv.*) and other respective metal ions (5 *equiv.*) under the identical conditions in ethanol. ((1) 1; (2) 1 + Mg^{2+}; (3) 1 + Al^{3+}; (4) 1 + Ba^{2+}; (5) 1 + Ca^{2+}; (6) 1 + Cd^{2+}; (7) 1 + Co^{2+}; (8) 1 + Cr^{3+}; (9) 1 + Cu^{2+}; (10) 1 + Fe^{2+}; (11) 1 + Fe^{3+}; (12) 1 + K^+; (13) 1 + Mn^{2+}; (14) 1 + Na^+; (15) 1 + Ni^{2+}; (16) 1 + Pb^{2+}; (17) 1 + Zn^{2+}) (λ_{ex} = 323 nm, slit: 3.0/3.0 nm).

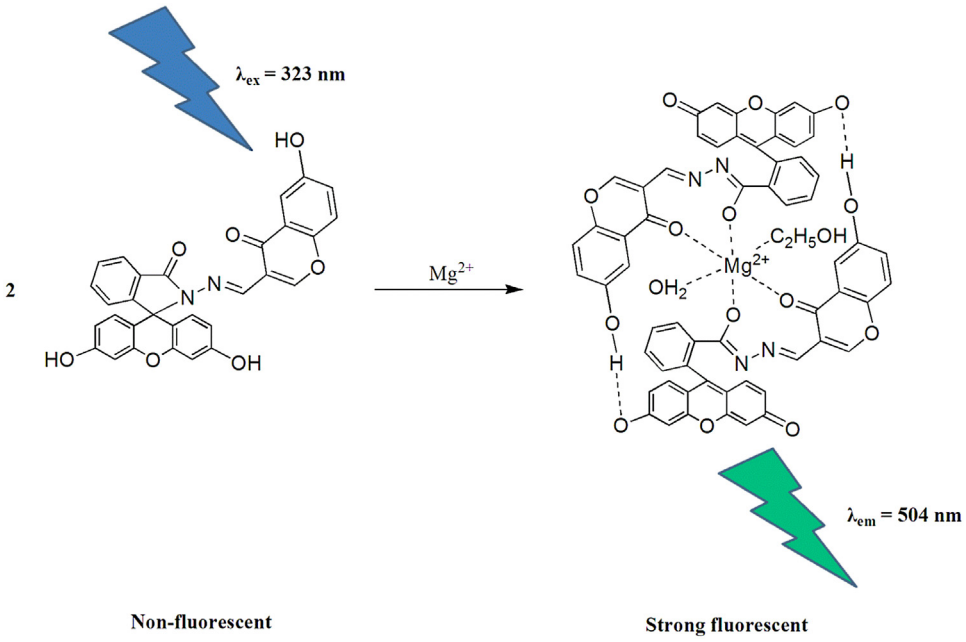

Scheme 2. The proposed binding mechanism for the response of 1 to Mg^{2+}.

plot and ESI–MS spectra that indicated 2: 1 stoichiometry, the binding constant (K) of compound **1** with Mg^{2+} was estimated as $5.62 \times 10^6\,M^{-1}$ by the Benesi–Hildebrand equation (1) from fluorescence titration experiment (Fig. S10), and the result was within the range 10^3–$10^9\,M^{-1}$ of those reported Mg^{2+} fluorescent probes [58–60].

A comparison between our fluorescent probe **1** and other previously reported probes for Mg^{2+} detection was listed in Table 1. In comparison with other fluorescent probes, our probe **1** had similar detection limit and binding constant value with that of others [61–63], and the detection of Mg^{2+} was not interfered from Ca^{2+}, indicating that **1** could recognize Mg^{2+} with high selectivity and sensitivity without interferences from most of other common metal ions.

3.5. ^1H NMR experiments

Finally, ^1H NMR experiments were studied to further investigate the binding mechanism for the response of **1** to Mg^{2+}. Fig. 7 shows the spectral changes of compound **1** upon addition of 1.0 *equiv.* of $Mg(NO_3)_2{\cdot}6H_2O$ in DMSO-*d*. Treatment of 1.0 *equiv.* of Mg^{2+} to the solution of compound **1** led to the considerable downfield shift in the proton signal of the hydroxy group from chromone from δ 10.14 ppm to δ 10.26 ppm and two proton signals of the hydroxy group from fluorescein from δ 9.95 ppm to δ 10.07 ppm, respectively, which indicated that two intramolecular hydrogen

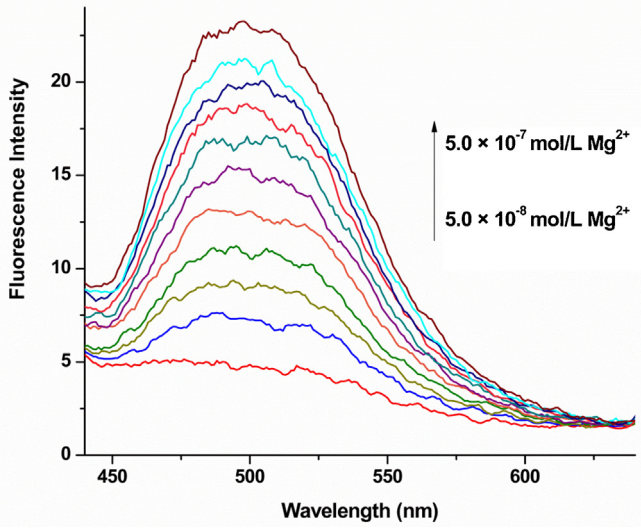

Fig. 4. Change in fluorescence emission spectra of 1 (50 μM) measured in ethanol upon addition of various concentration of Mg^{2+} (0.05, 0.10, 0.15, 0.20, 0.25, 0.30, 0.35, 0.40, 0.45, 0.50 μM, respectively) with an excitation at 323 nm.

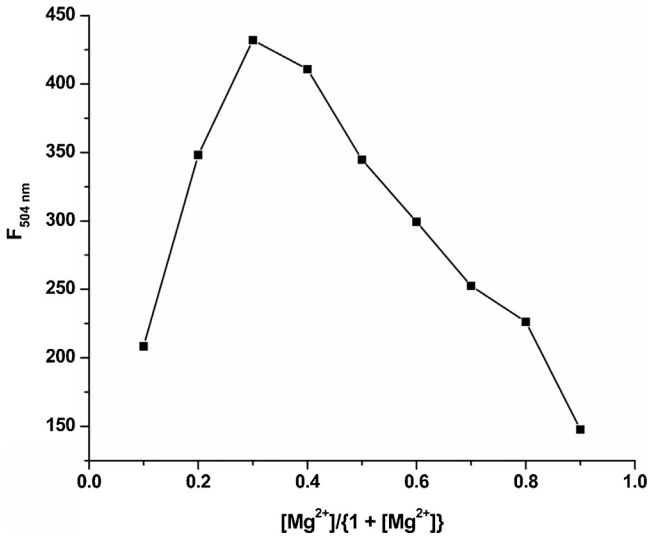

Fig. 5. Job's plot for determining the stoichiometry between 1 and Mg^{2+} in ethanol ($X_{Mg} = [Mg^{2+}]/([Mg^{2+}] + [1])$, the total concentration of 1 and Mg^{2+} was 100 μM).

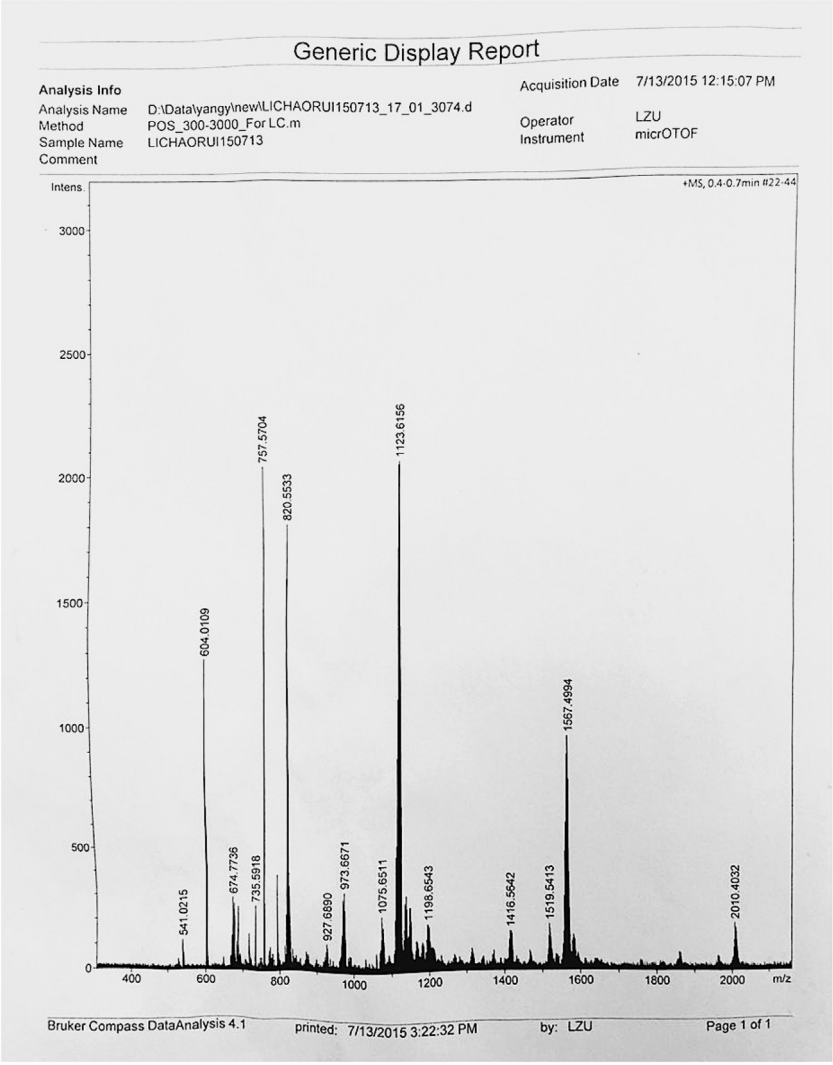

Fig. 6. ESI–MS spectra of 1 and Mg^{2+} in ethanol.

bonds were formed after complexation of compound **1** with Mg^{2+}. Additionally, the proton signal of the methenyl group (at δ 8.32 ppm) was shifted downfield to δ 8.36 ppm and the signal of the eighth proton H_8 of the chromone moiety (at δ 8.71 ppm) was shifted upfield to δ 8.65 ppm, respectively. However, almost no spectral changes were observed in other proton signals in the presence of Mg^{2+} (Fig. 7). From the results above, it was concluded that the oxygen atom of the carbonyl group from chromone moiety and the oxygen atom of the carbonyl group from the ring-opening structure of fluorescein moiety participated in the coordination of compound **1** with Mg^{2+}, and the ring-opening structure of the fluorescein moiety was observed in complex **1**-Mg^{2+}. In order to satisfy the coordination number of Mg^{2+} (CN = 6) [64–66], one hydrogen oxide molecule and one ethanol molecule were also coordinated with Mg^{2+} in the complex **1**-Mg^{2+} (Scheme 2), which was well consistent with the UV–vis titration spectra and ESI–MS spectra.

4. Conclusion

In summary, we designed and synthesized a novel fluorescein derivative **1** bearing the chromone moiety. This compound **1** could selectively bind with Mg^{2+} and responded to Mg^{2+} in the UV–vis and fluorescence emission spectra. The fluorescence emission intensity at 504 nm increased by about 49.58-fold in the presence of 0.5 *equiv.* of Mg^{2+} with high selectivity and sensitivity, for the detection limit could reach 2.67×10^{-8} M (0.64 ppb), and most metal ions that were abundant in human body did not interfere

Table 1
Comparison of the characteristics of probe 1 with those previously reported Mg^{2+} fluorescent probes.

Fluorescent probe	Interfering ions	Detection limit (M)	Binding constant (M^{-1})	Ref.
diethyl-2,2′-(3-nitro-2-oxochroman-4-ylazanediyl) diacetate	Ba^{2+}, Cs^{+}	5.00×10^{-8}	5.05×10^{5}	[58]
(*E*)-2-((2-pyridin-2-yl)hydrazono)methyl)quinolin-8-ol	Ca^{2+}, Cd^{2+}	1.91×10^{-8}	1.91×10^{7}	[59]
7-hydroxy-4-methyl-8-((pyridine-2-yl-imino)methyl)-2H-chromen-2-one	No interferences	9.00×10^{-8}	2.17×10^{4}	[60]
6-Hydroxy-3-formylchromone fluorescein hydrazone	Zn^{2+}	2.67×10^{-8}	5.62×10^{6}	This work

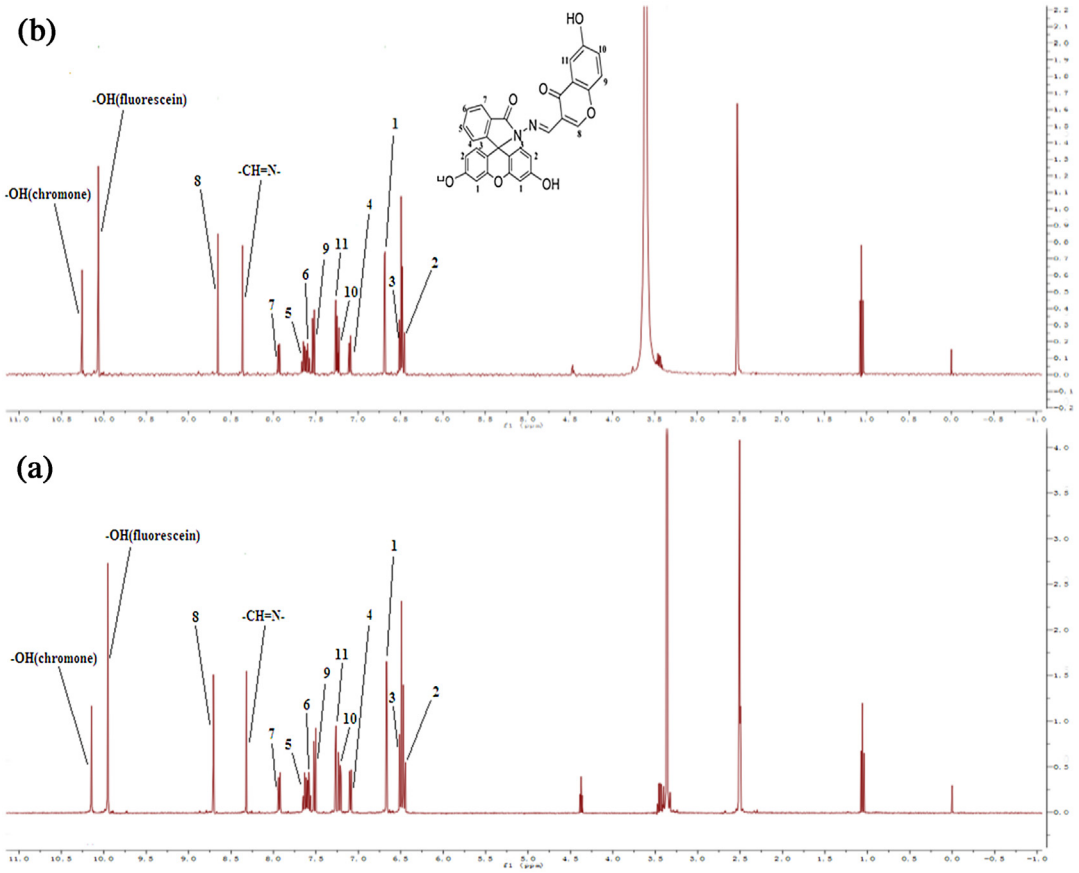

Fig. 7. ^{1}H NMR spectra of 1 upon addition of Mg^{2+} in DMSO-d_6 (a) 1; (b) 1 and Mg^{2+} (1.0 *equiv.*).

with the fluorescence response of **1** to Mg^{2+}. Furthermore, the reaction process between compound **1** and Mg^{2+} was nearly completed within 3 min, and the 2: 1 stoichiometry between compound **1** and Mg^{2+} was determined by fluorescence titration spectra, Job's plot and ESI–MS spectra. Therefore, this compound **1** could be utilized as a fluorescent probe for detecting and monitoring Mg^{2+} for real-time detection and might accelerate the development of other fluorescein-derived probes.

Acknowledgments

This work is supported by the National Natural Science Foundation of China (81171337). Gansu NSF(1308RJZA115).

Appendix A. Supplementary data

Supplementary data associated with this article can be found, in the online version, at http://dx.doi.org/10.1016/j.jphotochem.2016.03.001.

References

[1] A. Jasinski, M. Guzinski, G. Lisak, J. Bobacka, M. Bochenska, Solid-contact lead (II) ion-selective electrodes for potentiometric determination of lead(II) in presence of high concentrations of Na(I), Cu(II) Cd(II), Zn(II), Ca(II) and Mg(II), Sensor. Actuat. B-Chem. 218 (2015) 25–30.
[2] C. Perez-Rafols, N. Serrano, J.M. Diaz-Cruz, C. Arino, M. Esteban, Penicillamine-modified sensor for the voltammetric determination of Cd(II) and Pb(II) ions in natural samples, Talanta 144 (2015) 569–573.
[3] P. Jarujamrus, M. Amatatongchai, A. Thima, T. Khongrangdee, C. Mongkontong, Selective colorimetric sensors based on the monitoring of an unmodified silver nanoparticles (AgNPs) reduction for a simple and rapid determination of mercury, Spectrochim. Acta Part A Mol. Biomol. Spectrosc. 142 (2015) 86–93.
[4] S. Sahan, S. Sacmaci, A. Ulgen, S. Kartal, U. Sahin, A new automated system for the determination of Al(III) species in dialysis concentrates by electrothermal atomic absorption spectrometry using a combination of chelating resin, Microchem. J. 122 (2015) 57–62.
[5] N. Ozbek, S. Akman, Microwave plasma atomic emission spectrometric determination of Ca, K and Mg in various cheese varieties, Food Chem. 192 (2016) 295–298.
[6] J.J. Lee, H. Yoon, A comparative study of technological learning and organizational capability development in complex products systems: Distinctive paths of three latecomers in military aircraft industry, Res. Policy 44 (2015) 1296–1313.
[7] R. Shrivastava, J. Kaur, Studies on long lasting optical properties of Eu2+ and Dy3+ doped dibarium magnesium silicate phosphors, Chin. Chem. Lett. 26 (2015) 1187–1190.
[8] A. Lapresta-Fernandez, L.F. Capitan-Vallvey, Environmental monitoring using a conventional photographic digital camera for multianalyte disposable optical sensors, Anal. Chim. Acta. 706 (2011) 328–337.
[9] A.S. Hamdy, I. Doench, H. Mohwald, Smart self-healing anti-corrosion vanadia coating for magnesium alloys, Prog. Org. Coat. 72 (2011) 387–393.
[10] R.D. Grubbs, M.E. Maguire, Magnesium as a regulatory cation: criteria and evaluation, Magnesium 6 (1987) 113–127.
[11] C. Janning, E. Willbold, C. Vogt, J. Nellesen, A. Meyer-Lindenberg, H. Windhagen, F. Thorey, F. Witte, Magnesium hydroxide temporarily enhancing osteoblast activity and decreasing the osteoclast number in peri-implant bone remodeling, Acta. Biomater. 6 (2010) 1861–1868.
[12] A. Chaya, S. Yoshizawa, K. Verdelis, N. Myers, B.J. Costello, D.T. Chou, S. Pal, S. Maiti, P.N. Kumta, C. Sfeir, In vivo study of magnesium plate and screw degradation and bone fracture healing, Acta. Biomater. 18 (2015) 262–269.
[13] M.I. Martinez-Jimenez, S. Garcia-Gomez, K. Bebenek, G. Sastre-Moreno, P.A. Calvo, A. Diaz-Talavera, T.A. Kunkel, L. Blanco, Alternative solutions and new scenarios for translesion DNA synthesis by human PrimPol, DNA Repair 29 (2015) 127–138.

[14] S.S. Leonard, G.K. Harris, X.L. Shi, Metal-induced oxidative stress and signal transduction, Free Radical Bio. Med. 37 (2004) 1921–1942.
[15] M. Yasui, I. Yano, Y. Yase, K. Ota, Distribution of magnesium in central nervous system tissue, trabecular and cortical bone in rats fed with unbalanced diets of minerals, J. Neurol. Sci. 99 (1990) 177–183.
[16] G. Bhakta, V. Nurcombe, A. Maitra, A. Shrivastava, DNA-encapsulated magnesium phosphate nanoparticles elicit both humoral and cellular immune responses in mice, Res. Immunol. 4 (2014) 46–53.
[17] T.T. Zhao, B. Chen, H.P. Wang, R. Wang, H. Zhang, Evaluation of toxic and essential elements in whole blood from 0- to 6-year-old children from Jinan, China, Clin. Biochem. 46 (2013) 612–616.
[18] R. Moncayo, H. Moncayo, The WOMED model of benign thyroid disease: Acquired magnesium deficiency due to physical and psychological stressors relates to dysfunction of oxidative phosphorylation, BBA Clin. 3 (2015) 44–64.
[19] R. Moncayo, H. Moncayo, Exploring the aspect of psychosomatics in hypothyroidism: The WOMED model of body—mind interactions based on musculoskeletal changes psychological stressors, and low levels of magnesium, Woman-Psychosom. Gynaecol. Obst. 1 (2014) 1–11.
[20] C. Malpuech-Brugere, W. Nowacki, M. Daveau, E. Gueux, C. Linard, E. Rock, J.P. Lebreton, A. Mazur, Y. Rayssiguier, Inflammatory response following acute magnesium deficiency in the rat, BBA-Mol. Basis. Dis. 1501 (2000) 91–98.
[21] E. Mendez, A. Dieringer, S. Tao, M. Haigney, V. Pineiro-Carrero, T. Shea-Donohue, Magnesium (Mg2 +) deficiency induces inflammation and altered epithelial function in rat small intestine, Gastroenterology 114 (1998) A398.
[22] R.K. Rude, H.E. Gruber, Magnesium deficiency and osteoporosis: animal and human observations, J. Nutr. Biochem. 15 (2004) 710–716.
[23] X.R. Gao, M.D. Wang, X.Y. He, L.L. Tang, J.B. Liang, L.Y. Peng, H. Lin, H.W. Sun, H. Ma, J. Lin, Z.Y. Zuo, Decreased intralymphocytic magnesium content is associated with diastolic heart dysfunction in patients with essential hypertension, Int. J. Cardiol. 147 (2011) 331–334.
[24] M. Svagzdiene, E. Sirvinskas, D. Baranauskiene, D. Adukauskiene, Correlation of magnesium deficiency with C-reactive protein in elective cardiac surgery with cardiopulmonary bypass for ischemic heart disease, Medicinal 51 (2015) 100–106.
[25] L.C. Weng, N.J. Lee, W.T. Yeh, L.T. Ho, W.H. Pan, Lower intake of magnesium and dietary fiber increases the incidence of type 2 diabetes in Taiwanese, J. Formos. Med. Assoc. 111 (2012) 651–659.
[26] H. Nakagawa, M. Kano, S. Hasebe, T. Suzuki, N. Wakiyama, Real-time monitoring of lubrication properties of magnesium stearate using NIR spectrometer and thermal effusivity sensor, Int. J. Pharm. 441 (2013) 402–413.
[27] Z. Liu, C.N. Peng, Z.X. Lu, X.F. Yang, M.S. Pei, G.Y. Zhang, A novel fluorescent sensor derived from benzimidazo[2,1-a]benz[de] isoquinoline-7-one-12-carboxylic acid for Cu2+, Cd2+ and PPi, Dyes, Pigments 123 (2015) 85–91.
[28] Q.F. Niu, X.X. Wu, S.S. Zhang, T.D. Li, Y.Z. Cui, X.Y. Li, A highly selective and sensitive fluorescent sensor for the rapid detection of Hg2+ based on phenylamine-oligothiophene derivative, Spectrochim. Acta Part A Mol. Biomol. Spectrosc. 153 (2016) 143–146.
[29] X.H. Tian, X.F. Guo, L.H. Jia, R. Yang, G.Z. Cao, C.Y. Liu, A fluorescent sensor based on bicarboxamidoquinoline for highly selective relay recognition of Zn2+ and citrate with ratiometric response, Sens. Actuators B-Chem. 221 (2015) 923–929.
[30] V.K. Gupta, N. Mergu, L.K. Kumawat, A.K. Singh, Selective naked-eye detection of Magnesium (II) ions using a coumarin-derived fluorescent probe, Sens. Actuators B-Chem. 207 (2015) 216–223.
[31] J.C. Qin, Z.Y. Yang, L. Fan, B.D. Wang, b-Hydroxy-a-naphthaldehyde [2-(quinolin-8′-yloxy) acetyl] hydrazone as an efficient fluorescent chemosensor for Mg2+, Spectrochim. Acta Part A Mol. Biomol. Spectrosc. 140 (2015) 21–26.
[32] N. Singh, N. Kaur, R.C. Mulrooney, J.F. Callan, A ratiometric fluorescent probe for magnesium employing excited state intramolecular proton transfer, Tetrahedron Lett. 49 (2008) 6690–6692.
[33] C. Cheng, I.J. Reynolds, Subcellular localization of glutamate-stimulated intracellular magnesium concentration changes in cultured rat forebrain neurons using confocal microscopy, Neuroscience 95 (1999) 973–979.
[34] X.Q. Chen, K.H. Baek, Y. Kim, S.J. Kim, I. Shin, J. Yoon, A selenolactone-based fluorescent chemodosimeter to monitor mecury/methylmercury species in vitro and in vivo, Tetrahedron 66 (2010) 4016–4021.
[35] M. Dong, T.H. Ma, A.J. Zhang, Y.M. Dong, Y.W. Wang, Y. Peng, A series of highly sensitive and selective fluorescent and colorimetric off-on chemosensors for Cu (II) based on rhodamine derivatives, Dyes Pigments 87 (2010) 164–172.
[36] T.R. Li, Z.Y. Yang, Y. Li, Z.C. Liu, G.F. Qi, B.D. Wang, A novel fluorescein derivative as a colorimetric chemosensor for detecting copper(II) ion, Dyes Pigm. 88 (2011) 103–108.
[37] C. Queiros, A.M.G. Silva, S.C. Lopes, G. Ivanova, P. Gameiro, M. Rangel, A novel fluorescein-based dye containing a catechol chelating unit to sense iron(III), Dyes. Pigm. 93 (2012) 1447–1455.
[38] F.A. Abebe, E. Sinn, Fluorescein-based fluorescent and colorimetric chemosensors for copper in aqueous media, Tetrahedron Lett. 52 (2011) 5234–5237.
[39] D. Wang, X.Y. Xiang, X.L. Yang, X.D. Wang, Y.L. Guo, W.S. Liu, W.W. Qin, Fluorescein-based chromo-fluorescent probe for zinc in aqueous solution: Spirolactam ring opened or closed? Sens. Actuators B-Chem. 201 (2014) 246–254.
[40] E. Oliveira, J. Lorenzo, A. Cid, J.L. Capelo, C. Lodeiro, Non-toxic fluorescent alanine–fluorescein probe with green emission for dual colorimetric/fluorimetric sensing, J. Photochem. Photobio. A-Chem. 269 (2013) 17–26.
[41] X.D. Yu, P. Zhang, Q.R. Liu, Y.J. Li, X.L. Zhen, Y.M. Zhang, Z.C. Ma, An off–on fluorescent and colorimetric probe bearing fluorescein moiety for Mg2+ and Ca2 + via a controlled supramolecular approach, Mat. Sci. Eng. C. 39 (2014) 73–77.
[42] F.J. Huo, J.J. Zhang, Y.T. Yang, J.B. Chao, C.X. Yin, Y.B. Zhang, T.G. Chen, A fluorescein-based highly specific colorimetric and fluorescent probe for hypochlorites in aqueous solution and its application in tap water, Sens. Actuators B-Chem. 166–167 (2012) 44–49.
[43] R.T. Cummings, J.P. Dizio, G.A. Krafft, Photoactivable fluorophores. 2. Synthesis and photoactivation of functionalized 3-aroyl-2-(2-furyl)-chromones, Tetrahedron Lett. 29 (1988) 69–72.
[44] B.D. Wang, Z.Y. Yang, D.W. Zhang, Y. Wang, Synthesis structure, infrared and fluorescence spectra of new rare earth complexes with 6-hydroxy chromone-3-carbaldehyde benzoyl hydrazone, Spectrochim. Acta Part A Mol. Biomol. Spectrosc. 63 (2006) 213–219.
[45] Y.K. Jang, U.C. Nam, H.L. Kwon, I.H. Hwang, C. Kim, A selective colorimetric and fluorescent chemosensor based-on naphthol for detection of Al3+ and Cu2+, Dyes Pigm. 99 (2013) 6–13.
[46] T.J. Jia, W. Cao, X.J. Zheng, L.P. Jin, A turn-on chemosensor based on naphthol–triazole for Al(III) and its application in bioimaging, Tetrahedron Lett. 54 (2013) 3471–3474.
[47] G.L. Long, J.D. Winefordner, Limit of detection a closer look at the IUPAC definition, Anal. Chem. 55 (1983) 712A–724A.
[48] C.R. Lohani, J.M. Kim, S.Y. Chung, J. Yoon, K.H. Lee, Colorimetric and fluorescent sensing of pyrophosphate in 100% aqueous solution by a system comprised of rhodamine B compound and Al3+ complex, Analyst 135 (2010) 2079–2084.
[49] A.S. Dinca, C. Maxim, B. Cojocaru, F. Lloret, M. Julve, M. Andruh, A two-dimensional coordination polymer constructed from binuclear copper(II) metalloligands and manganese(II) ions: Synthesis, crystal structure and magnetic properties, Inorg. Chim. Acta. 440 (2016) 148–153.
[50] G.X. Xi, Y.B. Xi, Effects on magnetic properties of different metal ions substitution cobalt ferrites synthesis by sol–gel auto-combustion route using used batteries, Mater. Lett. 164 (2016) 444–448.
[51] S. Uysal, Z.E. Koc, Synthesis and characterization of dopamine substitue tripodal trinuclear [(salen/salophen/salpropen)M] (M = Cr(III), Mn(III), Fe(III) ions) capped s-triazine complexes: Investigation of their thermal and magnetic properties, J. Mol. Struct. 1109 (2016) 119–126.
[52] Y.P. Pan, S.L. Tian, X.R. Li, Y. Sun, Y. Li, G.R. Wentworth, Y.S. Wang, Trace elements in particulate matter from metropolitan regions of Northern China: Sources, concentrations and size distributions, Sci. Total. Environ. 537 (2015) 9–22.
[53] X.Q. Chen, T. Pradhan, F. Wang, J.S. Kim, J. Yoon, Fluorescent chemosensors based on spiroring-opening of xanthenes and related derivatives, Chem. Rev. 112 (2012) 1910–1956.
[54] H.J. Kim, J.E. Park, M.G. Choi, S. Ahn, S.K. Chang, Selective chromogenic and fluorogenic signalling of Hg2+ ions using a fluorescein-coumarin conjugate, Dyes Pigm. 84 (2010) 54–58.
[55] X.F. Yang, Y. Li, Q. Bai, A highly selective and sensitive fluorescein-based chemodosimeter for Hg2+ ions in aqueous media, Anal. Chim. Acta. 584 (2007) 95–100.
[56] J.G. Zhang, L. Zhang, Y.L. Wei, J. Ma, S.M. Shuang, Z.W. Cai, C. Dong, A selectively fluorescein-based colorimetric probe for detecting copper(II) ion: Spectrochim, Acta Part A Mol. Biomol. Spectrosc. 122 (2014) 731–736.
[57] U. Diwan, A. Kumar, V. Kumar, K.K. Upadhyay, P.K. Roychowdhury, A water compatible turn 'on' optical probe for Cu2+ based on a fluorescein-sugar conjugate, Sens. Actuators B-Chem. 196 (2014) 345–351.
[58] S. Devaraj, Y.K. Tsui, C.Y. Chiang, Y.P. Yen, A new dual functional sensor: Highly selective colorimetric chemosensor for Fe3+ and fluorescent sensor for Mg2+, Spectrochim. Acta Part A Mol. Biomol. Spectrosc. 96 (2012) 594–599.
[59] H. Hama, T. Morozumi, H. Nakamura, Novel Mg2+-responsive fluorescent chemosensor based on benzo-15-crown-5 possessing 1-naphthaleneacetamide moiety, Tetrahedron Lett. 48 (2007) 1859–1861.
[60] S.H. Mashraqui, S. Sundaram, A.C. Bhasikuttan, S. Kapoor, A.V. Sapre, Novel fluoroionophores incorporating diaryl-1,3,4-oxadiazole and aza-crown ring. Potentially sensitive Mg2+ ion sensor, Sens. Actuators B-Chem. 122 (2007) 347–350.
[61] M. Suresh, A. Das, New coumarin-based sensor molecule for magnesium and calcium ions, Tetrahedron Lett. 50 (2009) 5808–5812.
[62] M.H. Kao, T.Y. Chen, Y.R. Cai, C.H. Hu, Y.W. Liu, Y. Jhong, A.T. Wu, A turn-on Schiff-base fluorescence sensor for Mg2+ ion and its practical application, J. Lumin. 169 (2016) 156–160.
[63] S. Devaraj, Y.K. Tsui, C.Y. Chiang, Y.P. Yen, A new dual functional sensor: Highly selective colorimetric chemosensor for Fe3+ and fluorescent sensor for Mg2+, Spectrochim. Acta Part A Mol. Biomol. Spectrosc. 96 (2012) 594–599.
[64] D.S. Raja, J.H. Luo, T.G. Chang, S.H. Lo, C.Y. Wu, C.H. Lin, Solvothermal synthesis, crystal structures and properties of two new magnesium coordination polymers of (L)-malic acid, Inorg. Chem. Commun. 32 (2013) 22–27.
[65] P.J. Calderone, D. Banerjee, A.C. Santulli, S.S. Wong, J.B. Parise, Synthesis characterization, and luminescence properties of magnesium coordination networks using a thiophene-based linker, Inorg. Chim. Acta. 378 (2011) 109–114.
[66] N. Ghosh, T. Chakraborty, S. Mallick, S. Mana, D. Singha, B. Ghosh, S. Roy, Synthesis, characterization and study of antioxidant activity of quercetin-magnesium complex, Spectrochim. Acta Part A Mol. Biomol. Spectrosc. 151 (2015) 807–813.